

## ELECTROCHEMICAL BEHAVIOUR OF EXPERIMENTAL Ti30Ta ALLOY IN THE PRESENCE OF FLUORIDE AND ALBUMIN PROTEIN

R. CHELARIU<sup>a</sup>, D. MARECI<sup>b</sup>, C. MUNTEANU<sup>c</sup>, G. BOLAT<sup>b</sup>, C. CRIMU<sup>c</sup>, I. ZETU<sup>d\*</sup>

<sup>a</sup>The "Gheorghe Asachi" Technical University of Iasi, Faculty of Materials Science and Engineering, 41 Prof. dr. doc. D. Mangeron St., 700050, Iasi, Romania

<sup>b</sup>The "Gheorghe Asachi" Technical University of Iasi, Faculty of Chemical Engineering and Environmental Protection, 73 Prof. dr. doc. D. Mangeron St., 700050, Iasi, Romania

<sup>c</sup>The "Gheorghe Asachi" Technical University of Iasi, Faculty of Mechanical Engineering, 61-63 Prof. Dr. Doc. D. Mangeron St., 700050, Iasi, Romania

<sup>d</sup>Grigore T. Popa University of Medicine and Pharmacy, Faculty of Dentistry, Universitatii Street no. 16, 700115 Iasi, Romania

Electrochemical behaviour of the studied Ti30Ta together with the currently used commercial pure titanium (cp-Ti) was investigated for dental applications by electrochemical impedance spectroscopy (EIS). Acidified (pH = 4.5) fluoridated artificial saliva (0.3 wt.% NaF) was employed as aggressive solution. Because the proteins have a role on the passivation of metals, the effect of albumin proteins addition in acidified fluoridated artificial saliva on the electrochemical behaviour of cp-Ti and Ti30Ta was studied. Compared to cp-Ti, Ti30Ta alloy show larger impedances which can be associated with good stability of passive layer in acidified fluoridated artificial saliva with and without albumin protein. The equivalent circuits (ECs) simulating the electrochemical behaviour of cp-Ti and Ti30Ta alloy in acidified fluoridated artificial saliva with and without albumin protein were proposed. The presence of albumin protein in acidified fluoridated artificial saliva improved the corrosion resistance of the both Ti sample. The surface morphology of the both samples was studied using scanning electron microscopy (SEM). The experimental results confirm that the presence of Ta in the Ta30Ta alloy has a beneficial effect on its behaviour in acidified fluoridated artificial saliva with and without albumin protein.

(Received August 8, 2014; Accepted October 15, 2014)

*Keywords:* Ti30Ta alloy, Albumin protein, EIS, Corrosion resistance, SEM

### 1. Introduction

Actually, metallic biomaterials used in biomedical applications include stainless steel, cobalt-chromium based and titanium alloys. The main limitation of these metallic materials is the release of the toxic metallic ion that can lead to various adverse tissue reactions.

Because cp-Ti (commercial pure titanium) and its alloys exhibit a high specific ration, good corrosion resistance and biocompatibilities have attracted a great deal of attention for biomedical application.

Ti materials are grouped into  $\alpha$ -type, ( $\alpha + \beta$ )-type, and  $\beta$ -type alloys. Mo, V, Nb, Ta are  $\beta$ -stabilizers elements which decrease the temperature of allotropic transformation, forming continuous series of solid solution with  $\beta$ -type Ti alloys. V is unsuitable for biomedical application due to their toxicity to human body. Moreover, some elements including Ti, Ta, Nb, and Zr are

---

\*Corresponding author: nicoleta.zetu@gmail.com

known as valve metals [1, 2] to form a thin oxidation layer on their surface with high corrosion resistance, so they are considered to be bioinert materials. Thus, new Ti alloys using Nb, Ta, Zr and Mo as alloying elements ( $\beta$ -stabilizer elements) have been developed [3-12].

Ta offers superior corrosion resistance over most other metals, high biocompatibility in human body [13] but have a relatively high cost.

In the mouth, dental metallic materials may come in contact with fluoride compounds from toothpastes, mouth rinses, orthodontic gels, dietary supplements or drinking water [14]. Some authors [15-19] have found that F<sup>-</sup> ions affect the corrosion behaviour of Ti and its alloys.

Furthermore, some reports have shown that the presence of protein may have negative [20] or positive influence [21-23] on the corrosion resistance of Ti and its alloys.

Electrochemical impedance spectroscopy (EIS) techniques have been used in a number of studies on the corrosion of dental materials and EIS spectra differ in shape and in the numerical values [24-28]. EIS is particularly useful when monitoring some electrochemical change as a function of time, being a non-destructive technique.

The aim of the present study was to compare the electrochemical properties of the Ti30Ta alloy with those of commercial pure titanium (cp-Ti) as a function of time immersion in acidified fluoridated artificial saliva with and without albumin protein.

## 2. Materials and methods

The electrochemical tests were conducted employing Ti30Ta alloy (30 wt.% Ta) and cp-Ti (99.9 wt.% Ti). The Ti30Ta alloy was synthesized by cold crucible levitation melting technique in a high frequency induction furnace under a pure Ar atmosphere. The cp-Ti samples were obtained from a bar stock in annealed state.

The microstructure of both Ti based materials were examined using a LEICA DMI5000 M metallographic microscope equipped with a dedicated digital camera connected to a personal computer and analyzed with the Leica Application Suite software program. Prior to optical imaging, the samples were first mechanically abraded using a sequence of silicon carbide abrasive papers followed by a final polishing step with 0.3  $\mu\text{m}$  alumina suspension. Next, the samples were cleaned in alcohol and distilled water using an ultrasonic bath, and finally etched in a solution containing 5 wt.% HNO<sub>3</sub>, 5 wt.% HF and the balance in H<sub>2</sub>O.

The microstructure of both Ti materials is shown in Fig. 1.

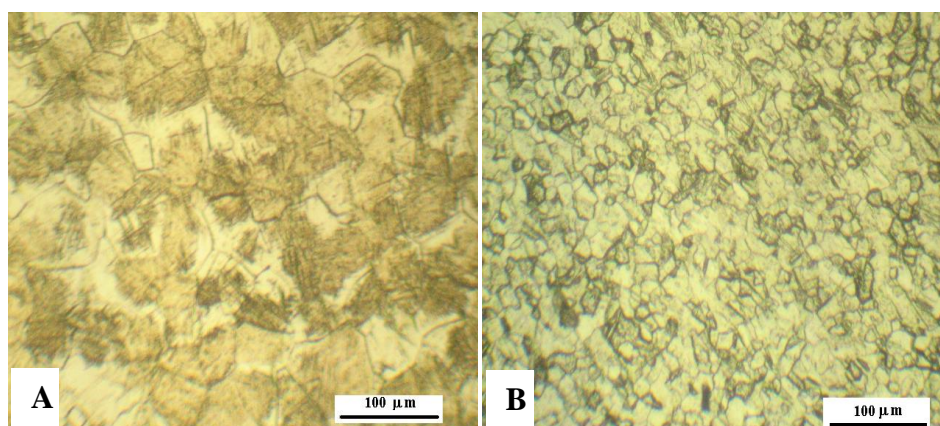


*Fig. 1. Optical micrographs of the surface of: (A) Ti30Ta alloy, and (B) cp-Ti used in electrochemical study.*

The Ti30Ta alloy (Fig. 1A) had a ( $\alpha + \beta$ ) duplex microstructure which consists in an acicular  $\alpha$ -phase formed within primary  $\beta$  grains. For cp-Ti, as shown in Fig. 1B, the microstructure is characterized by the presence of  $\alpha$ -Ti equiaxed grain.

The solution used for electrochemical test consisted of Fusayama artificial saliva [29] with 0.3 wt.% NaF. The pH of the test solution was adjusted to 4.5 by lactic acid in order to accentuate corrosion process. The lactic acid attained a content that is specific for medium existing under dental plaque [30].

Also, to evaluate the effect of albumin protein on the electrochemical behaviour of cp-Ti and Ti30Ta a albumin protein concentration of 0.6 wt.% was added to the acidified fluoridated artificial saliva. The concentration of proteins in the saliva may vary from less than 1 to more than 0.6 wt.% [31].

The test specimens were placed in a glass corrosion flow cell kit (C145/170, Radiometer, France) [32], which were filled with both acidified fluoridated artificial saliva with and without albumin protein. A saturated calomel electrode was used as the reference electrode, and a platinum coil as the counter electrode. The potentials in this paper are reported versus the saturated calomel electrode (SCE). The temperature of the electrochemical cell was maintained at  $37 \pm 1$  °C.

Electrochemical measurements were performed using a potentiostat model PARSTAT 4000 (Princeton Applied Research, NJ, USA). The instrument was controlled by a personal computer and *VersaStudio* software. Prior to testing, the working electrodes were mechanically abraded using emery paper up to 2000 grit, next polished with 0.3  $\mu\text{m}$  alumina suspension, ultrasonically cleaned in acetone and deionized water, and finally dried in open air.

Electrochemical impedance spectra were measured over a frequency range extending from 100 kHz to 10 mHz using a 10 mV amplitude AC voltage signal. The EIS tests were recorded at the open circuit potential developed by the samples after 10 min ( $0.6 \cdot 10^3$  s), 1 hour ( $3.6 \cdot 10^3$  s), and 8 hours ( $28.8 \cdot 10^3$  s) of immersion in both test solutions. Analysis of the spectra was performed in terms of equivalent circuit (EC) fitting using *ZSimpWin* software.

The surface morphology of both Ti based samples after 8 hours exposure times in acidified fluoridated artificial saliva with and without albumin protein was assessed using scanning electron microscopy (SEM; Quanta 3D, FEI, Hillsboro, OR, USA).

### 3. Results and discussion

For a given environment, corrosion depends on the structure and composition of the material sample. The alloys of the present study have different chemical compositions, and different structure.

The electrochemical characteristics of the oxidized alloys were quantified using electrochemical impedance spectroscopy (EIS). The EIS experiments were carried out at stationary conditions. The EIS results are presented in the form of Nyquist plots in which the imaginary impedance ( $Z_{im}$ ) is plotted against the real impedance ( $Z_{re}$ ). Figure 2(A-B) shows the Nyquist plots obtained for both cp-Ti and Ti30Ta samples, at open circuit potential, after 10 min, 1 hour, and 8 hours of immersion in acidified fluoridated artificial saliva.

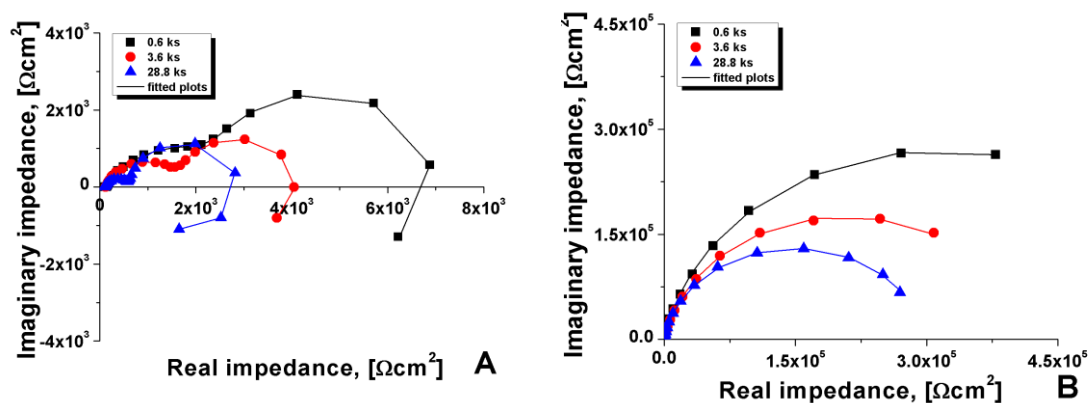


Fig. 2. Measured (discrete points) and fitted (solid lines) Nyquist impedance spectra for: (A) cp-Ti, and (B) Ti30Ta alloy during different times exposure at acidified fluoridated artificial saliva, at 37 °C.

The Nyquist plot of cp-Ti shows two capacitive semicircles in the high and intermediate frequency followed by an inductive arc in the low frequency range for all three immersion times. The first capacitive arc related the charge transfer process and a second semicircle present at intermediate frequencies related the corrosion products layer.

For the Ti30Ta alloy in acidified fluoridated artificial saliva (Fig. 2B), the impedance spectra was characterized by one large semicircle (one capacitive loop).

Bode spectra recorded at open circuit potential, with the cp-Ti and Ti30Ta samples for a different period of time immersion in acidified fluoridated artificial saliva, at 37 °C, are shown in Figure 3(A-B). The advantages of this procedure are that the data for all measured frequencies are shown and a wide range of impedance values can be displayed simultaneously. The frequency dependence of the impedance modulus and the phase shift indicate whether one or more time constants are present in the system.

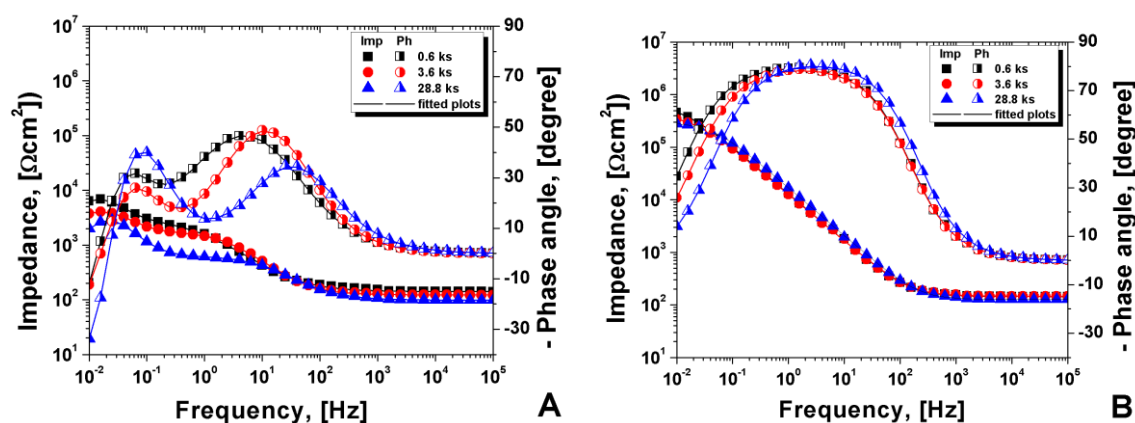


Fig. 3. Measured (discrete points) and fitted (solid lines) Bode impedance spectra for (A) cp-Ti, and (B) Ti30Ta alloy after different time immersion in acidified fluoridated artificial saliva, at 37 °C.

In the case of cp-Ti, Bode phase plots show two relaxation time constants, i.e., two peaks are observed in the Bode phase plots. Smaller impedance values were measured, together with the observation of an inductive behaviour of the system in the low frequency. Analysis of Bode spectra in terms of an equivalent circuit (EC) allowed the values of the impedance parameters. The EC employed to model the system parameters is depicted in Fig. 4A, and the fitted parameters are given in Table 1. The physical meaning of the given circuit is the association of the corrosion product layer /electrolyte interface ( $R_1Q_1$ ) with the corrosion product layer itself ( $R_2Q_2$ ). The experimental data show good fitting and an error smaller than 5%.

Constant phase elements (CPE) were used instead of pure capacitances because of the non-ideal capacitive response due to the distributed relaxation feature of the passive oxide layer thermal generated. The impedance representation of CPE is given by:

$$Z_{\text{(CPE)}} = \frac{1}{Y_0(j\omega)^n} \quad (1)$$

where  $\omega$  is the angular frequency and  $Y_0$  is a constant, and the value of the exponent  $n$  indicates the deviation from ideal capacitive behaviour (e.g., when  $n = 1$ ).

$R_{\text{sol}}$  is the resistance of solution occurring between the sample and the reference electrode. This parameter has a value around 70  $\Omega \text{ cm}^2$ , in acidified fluoridated artificial saliva and is not listed in Table 1.

Table 1. Electrochemical parameters obtained from EIS spectra using the selected ECs for the Ti samples after different immersion time in acidified fluoridated artificial saliva (pH = 4.5) with 0.3 wt.% NaF, at 37 °C

Titanium samples	Immersion time	$10^5 Q_1 / S \text{ cm}^{-2} \text{ s}^n$	$n_1$	$10^{-4} R_1 / \Omega \text{ cm}^2$	$10^4 Q_2 / S \text{ cm}^{-2} \text{ s}^n$	$n_2$	$10^{-3} R_2 / \Omega \text{ cm}^2$
cp-Ti	10 minutes	75.3	0.83	0.09	2.5	0.81	5.9
	1 hour	86.8	0.83	0.08	3.7	0.80	4.1
	8 hours	93.6	0.81	0.05	5.6	0.80	1.9
Ti30Ta	10 minutes	1.4	0.89	48.4	-	-	-
	1 hour	1.4	0.89	41.6	-	-	-
	8 hours	1.5	0.89	32.7	-	-	-

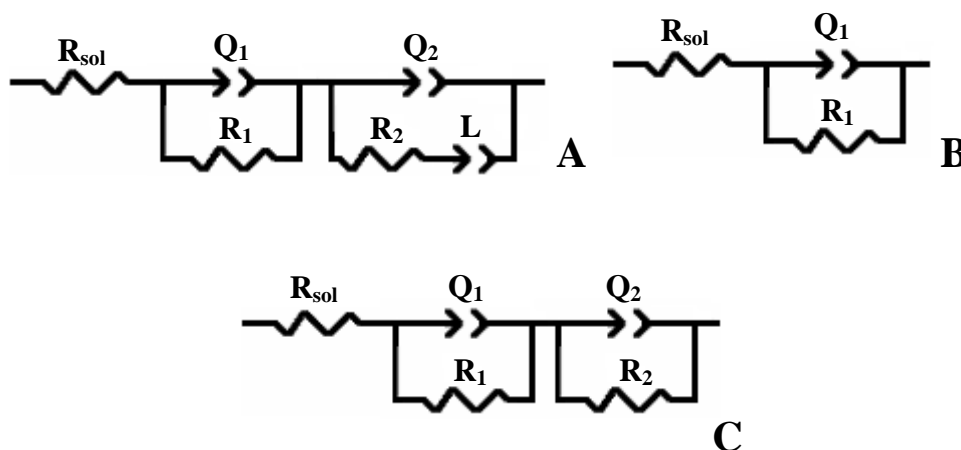


Fig. 4. Equivalent circuits (ECs) used for the interpretation of the measured impedance spectra.

The high frequency  $R_1$  and  $Q_1$ , parameters describe charge transfer resistance and double layer constant phase element and  $R_2$  and  $Q_2$  parameters describe the resistance and the constant phase elements of the corrosion products layers. The occurrence of the inductive combination  $R_2L$  is attributed to the relaxation of the corrosion products formed on the cp-Ti surface. The very low values of the charge transfer resistance ( $R_1$ ) reveal the dissolution of cp-Ti in acidified fluoridated artificial saliva without albumin protein. Also, the  $R_2$  decrease by increasing the immersion time. These results indicate the corrosion products dissolution causing the decrease of the total system impedance. The presences of fluoride ions in solution alter the structure of the oxide layer spontaneously formed in air causing it to be porous. Major corrosion occurred when the cp-Ti was immersed in acidified fluoridated artificial saliva.

The impedance spectra found for Ti30Ta alloy (Fig. 3B) exhibited a near capacitive response illustrated by a phase angle close to  $-80^\circ$  over a wide frequency range.

Bode phase spectra of Ti30Ta alloy for a different period of time immersion in acidified fluoridated artificial saliva can be described by one time constant. For this reason, experimental data can be fitted using an EC presented in Fig. 4B. The EC consists of the parallel combination terms ( $R_1Q_1$ ) in series with the resistance of the solution ( $R_{sol}$ ) occurring between the sample and the reference electrode. The parameters  $R_1$  and  $Q_1$  describe the properties of the passive films formed on this alloy, respectively the resistance and constant phase element of the passive layers. The elements circuit obtained by the fitting procedure is also shown in Table 1. When a protective surface layer is formed on metal, the metal impedance predominantly corresponds to the capacitive effect, and the charge transfer reaction is relatively smaller. Although,  $R_1$  decrease slowly with

time showing that the native oxide layer formed on Ti30Ta alloy is corrosion resistant. The acidified fluoridated artificial saliva presents a harmful effect on this passive layer as the immersion time increases. However, the resistance of passive layer of Ti30Ta immersed 8 hours in acidified fluoridated artificial saliva is large (order of  $10^5 \Omega \text{ cm}^2$ ).

Figure 5(A-B) shows Nyquist diagram for the cp-Ti and Ti30Ta alloy in the acidified fluoridated artificial saliva containing albumin protein after different immersion times.

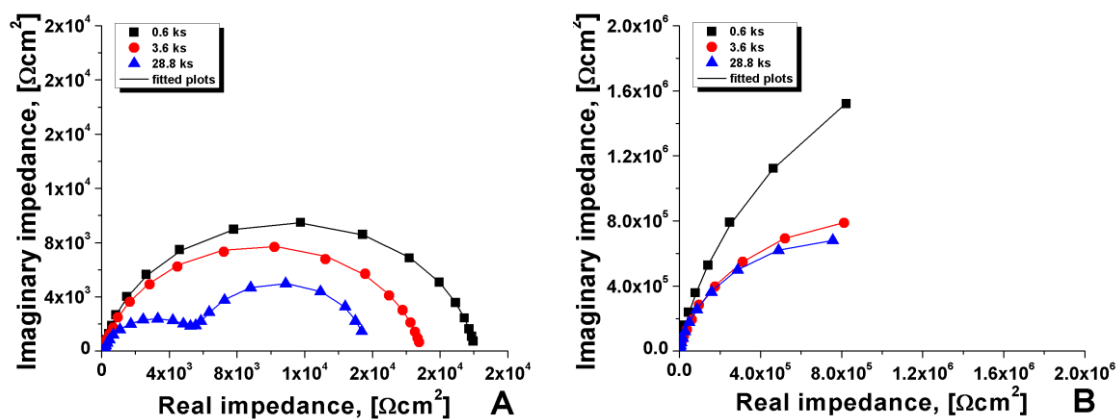


Fig. 5. Measured (discrete points) and fitted (solid lines) impedance spectra for: (A) cp-Ti, and (B) Ti30Ta alloy during different times exposure at acidified fluoridated artificial saliva with 0.6 wt.% albumin protein, at  $37^\circ\text{C}$ .

The Nyquist diagram for cp-Ti (Fig. 5A) shows a capacitive arc in the intermediate and low frequency for short-term immersion times in acidified fluoridated artificial saliva with albumin protein (10 min and 1 hour). For 8 hours immersion time a second capacitive arc appears. For the Ti30Ta alloy in acidified fluoridated artificial saliva with albumin protein (Fig. 5B) the impedance spectra showing one large capacitive arc.

Fig. 6(A-B) depicts the Bode impedance plots for cp-Ti and the T30Ta alloy under open circuit potential conditions in acidified fluoridated artificial saliva with albumin protein after different exposure times, at  $37^\circ\text{C}$ .

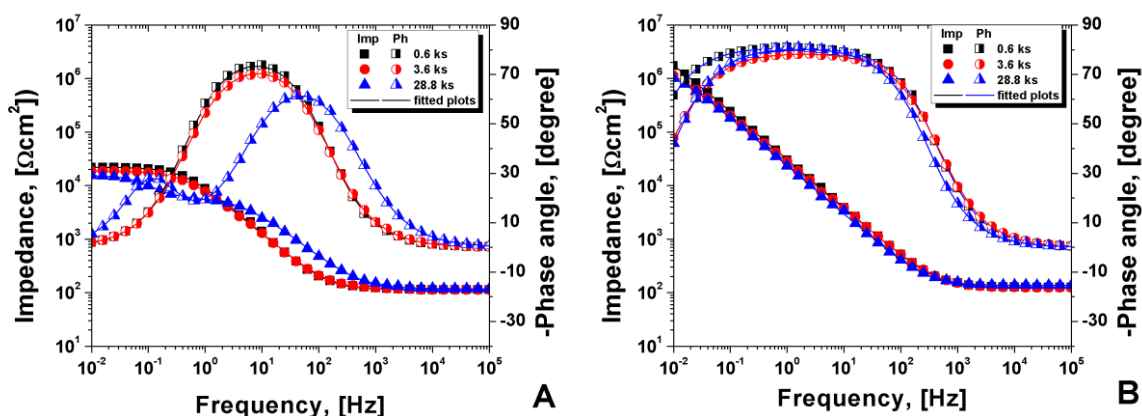


Fig. 6. Measured (discrete points) and fitted (solid lines) Bode impedance spectra for (A) cp-Ti, and (B) Ti30Ta alloy after different time immersion in acidified fluoridated artificial saliva with albumin protein, at  $37^\circ\text{C}$ .

One peak observed in Bode phase diagram for cp-Ti after 10 min and 1 hour immersion times in acidified fluoridated artificial saliva with albumin protein indicates the involvement of

one relaxation time constant. Simple EC comprised of one time constant (Fig. 4B) was used to model the experimental spectra. The values of fitted parameters of the EC for cp-Ti after a 10 min and 1 hour immersion in the acidified fluoridated artificial saliva with albumin protein are presented in Table 2.

*Table 2. Electrochemical parameters obtained from EIS spectra using the selected ECs for the Ti samples after different immersion time in acidified fluoridated artificial saliva with 0.6 wt.% albumin protein, at 37 °C*

Titanium samples	Immersion time	$10^5 Q_1 / S \text{ cm}^{-2} \text{ s}^n$	$n_1$	$10^{-4} R_1 / \Omega \text{ cm}^2$	$10^4 Q_2 / S \text{ cm}^{-2} \text{ s}^n$	$n_2$	$10^{-4} R_2 / \Omega \text{ cm}^2$
cp-Ti	10 minutes	1.6	0.85	2.4	-	-	-
	1 hour	1.6	0.84	1.9	-	-	-
	8 hours	23.1	0.81	0.2	6.4	0.80	1.1
Ti30Ta	10 minutes	0.8	0.90	156	-	-	-
	1 hour	0.9	0.89	132	-	-	-
	8 hours	0.9	0.88	107	-	-	-

Again,  $R_1$  and  $Q_1$ , parameters describe charge transfer resistance and double layer constant phase element. The same value for  $R_{\text{sol}}$  (around  $70 \Omega \text{ cm}^2$ ) was observed in experimental studies and it is not listed in Table 2.

The Bode-phase spectra of the cp-Ti recorded after 8 hours immersion in the acidified fluoridated artificial saliva with albumin protein revealed two time constants. The experimental data can be satisfactorily fitted with the equivalent circuit shown in Fig. 4C, and the values of fitted parameters are presented in Table 2. The new components in the EC,  $R_2$  and  $Q_2$  are the resistance and the constant phase element associated with the corrosion products layer.

From the Bode phase plots of Ti30Ta alloy in acidified fluoridated artificial saliva with albumin protein one peak was observed indicates the involvement of one relaxation time constant. The EIS spectra were fitted and the same model presented in Fig. 4B was proposed.

The presence of 0.6 wt.% albumin protein in the acidified fluoridated artificial saliva (pH = 4.5) increased the impedance of both Ti samples compared to that without albumin protein addition (Figure 5 and 6). Also, the electrochemical data presented from Tables 1 and 2 suggest that the albumin protein increasing the corrosion resistance of both samples. The deterioration of the passive film can be avoided by the adsorption of albumin protein onto sample surface [33].

However, the corrosion resistances of both Ti samples decrease with immersion times. This can be explained by the competition between adsorption of albumin protein on to the sample surface and dissolution of oxide layer [34].

In terms of EIS analysis, the addition of Ta as alloying element in large percentage (30 wt.%) improve corrosion resistance in acidified fluoridated artificial saliva with and without albumin protein.

The surface topography of cp-Ti and Ti30Ta alloy samples after 8 hours immersion times in acidified fluoridated artificial saliva were examined by scanning electron microscopy (SEM) and are displayed in Figure 7(A-B).

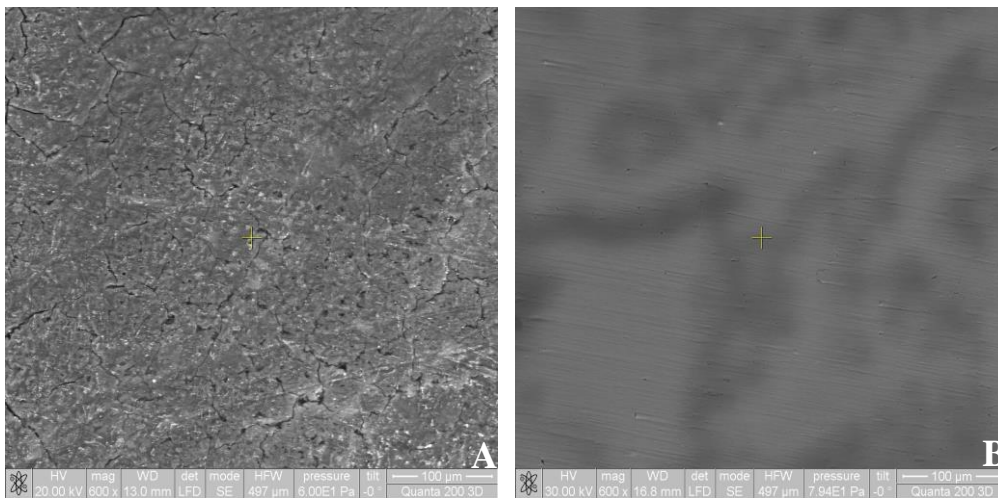
Surface analysis of cp-Ti after 8 hours immersion times in acidified fluoridated artificial saliva indicated a notable general degradation.

For Ti30Ta alloy a uniform corrosion were observable when acidified fluoridated artificial saliva was used for EIS tests.

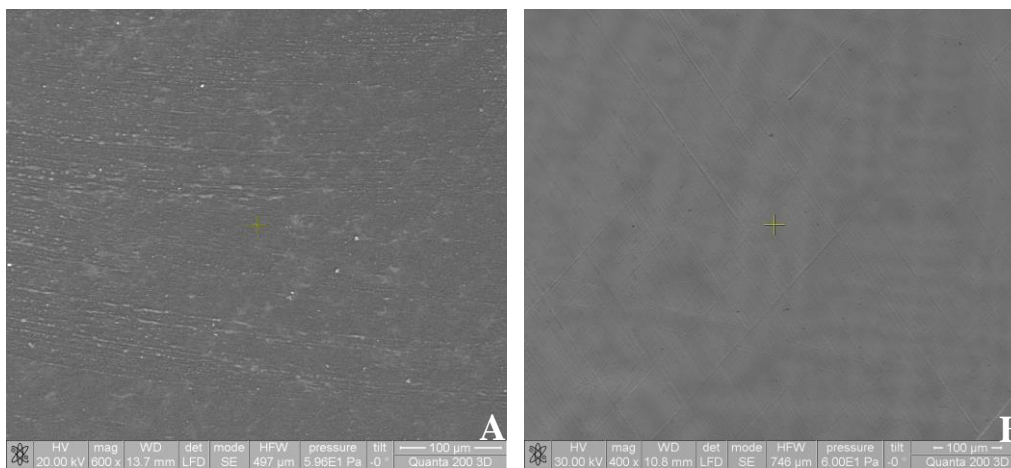
SEM images, after 8 hours immersion times in acidified fluoridated artificial saliva with 0.6 wt.% albumin protein addition are shown in Fig. 8(A-B).

Figure 8A indicates that the surface of cp-Ti is rougher. Therefore, the oxide layer spontaneously formed in air on the cp-Ti cannot protect this material from corrosion after 8 hours exposure times in acidified fluoridated artificial saliva with 0.6 wt.% albumin protein. No visible

signs of deterioration appeared on the Ti30Ta alloy surface except the presence of polishing scratches.



*Fig. 7. SEM micrographs for: (A) cp-Ti, and (B) Ti30Ta alloy after 8 hours exposure times in acidified fluoridated artificial saliva at 37 °C.*



*Fig. 8. SEM micrographs for: (A) cp-Ti, and (B) Ti30Ta alloy after 8 hours exposure times in acidified fluoridated artificial saliva with 0.6 wt.% albumin protein at 37 °C.*

#### 4. Conclusions

Electrochemical impedance spectroscopy is a very useful technique for studying the corrosion behaviour of metallic biomaterials. The analysis of the electrochemical impedance parameters reveal that the cp-Ti and Ti30Ta alloy do not behave in the same way. The resistances of passive layer obtained from EIS spectra slowly decreases with immersion time in acidified fluoridated artificial saliva with and without albumin protein for Ti30Ta alloy, but remain large ( $10^5 - 10^6 \Omega \text{ cm}^2$ ). The Ti30Ta alloy surface is initially covered by an air spontaneously formed oxide film, which acts as a barrier rendering the alloy dissolution more difficult. In the case of cp-Ti, EIS measurements showed that corrosion process was under charge transfer control. The EIS results exhibited small impedance values (order  $10^3 - 10^4 \Omega \text{ cm}^2$ ) obtained from medium to low frequency indicating the dissolution process of oxide layer spontaneously formed on cp-Ti.

The presence of 0.6 wt.% albumin protein in acidified fluoridated artificial saliva (pH = 4.5) with 0.3 wt.% NaF increase the corrosion resistance of both sample confirming the adsorption process of protein albumin on to metallic surface.

Presence of 30 wt.% Ta in the Ti alloy is responsible for better corrosion resistance performance.

### Acknowledgements

This work was supported by a grant of the Romanian National Authority for Scientific Research, CNCS-UEFISCDI, project number PN-II-ID-PCE-2011-3-0218.

### References

- [1] A. Davydov, *Electrochim. Acta* **46**, 3777 (2001).
- [2] O. E. Linarez Perez, V. C. Fuertes, M. A. Perez, M. Lopez Teijelo, *Electrochem. Commun.* **10**, 433 (2008).
- [3] L. M. Elias, S. G. Schneider, S. Schneider, H. M. Silva, F. Malvisi, *Mater. Sci. Eng. A* **432**, 108 (2006).
- [4] T. Gloriant, G. Texier, F. Prima, D. Laillé, D. M. Gordin, I. Thibon, D. Ansel, *Adv. Eng. Mater.* **8**, 961 (2006).
- [5] N. T. C. Oliveira, S. R. Biaggio, P. A. P. Nascente, S. Piazza, C. Sunseri, F. Di Quarto, *Electrochim. Acta* **51**, 3506 (2006).
- [6] M. Niinomi, *J. Mech. Behav. Biomed. Mater.* **1**, 30 (2008).
- [7] S. L. Assis, S. Wolyneć, I. Costa, *Mater. Corros.* **59**, 739 (2008).
- [8] D. Mareci, R. Chelariu, G. Ciurescu, D. Sutiman, D. M. Gordin, T. Gloriant, *J. Optoelectron. Adv. Mater.* **12**, 1590 (2010).
- [9] D. Mareci, R. Chelariu, I. Dan, D. M. Gordin, T. Gloriant, *J. Mater. Sci.-Mater. Med.* **21**, 2907 (2010).
- [10] D. Mareci, R. Chelariu, G. Bolat, A. Cailean, D. Sutiman, *J. Optoelectron. Adv. Mater.* **14**, 112 (2012).
- [11] G. Bolat, D. Mareci, R. Chelariu, J. Izquierdo, S. González, R. M. Souto, *Electrochim. Acta* **113**, 470 (2013).
- [12] R. Chelariu, G. Bolat, J. Izquierdo, D. Mareci, D. M. Gordin, T. Gloriant, R. M. Souto, *Electrochim. Acta* **137**, 280 (2014).
- [13] E. Eisenbarth, D. Velten, M. Muller, R. Thull, J. Breme, *Biomaterials* **22**, 5705 (2001).
- [14] G. Mabilieu, S. Bourdon, M. L. Joly-Guillou, R. Filmon, M. F. Basle, D. Chappard, *Acta Biomater.* **2**, 121 (2006).
- [15] L. Reclaru, J. M. Meyer, *Biomaterials* **19**, 85 (1998).
- [16] N. Schiff, B. Grosgeat, M. Lissac, F. Dalard, *Biomaterials* **23**, 1995 (2002).
- [17] L. Tzu-Hsin, W. Chia-Ching, H. Ta-Ko, C. Li-Kai, C. Ming-Yung, H. Her-Hsiung, *J. Alloys Compd.* **488**, 482 (2009).
- [18] A. M. Al-Mayouf, A. A. Al-Swayih, N. A. Al-Mobarak, *Mater. Corros.* **55**, 88 (2004).
- [19] S. Kumar, T. Narayanan, S. S. Kumar, *Corros. Sci.* **52**, 1721 (2010).
- [20] M. A. Khan, R. L. Williams, D. F. Williams, *Biomaterials* **20**, 765 (1999).
- [21] K. Ide, M. Hattori, M. Yoshinari, E. Kawada, Y. Oda, *Dent. Mater. J.* **22**, 359 (2003).
- [22] H. Her-Hsiung, L. Tzu-Hsin, *Dent. Mater.* **21**, 749 (2005).
- [23] D. Mareci, R. Chelariu, G. Ciurescu, D. Sutiman, T. Gloriant, *Mater. Corros.* **61**, 768 (2010).
- [24] B. B. Zhang, Y. E. Zheng, Y. Liu, *Dent. Mater.* **25**, 672 (2009).
- [25] A. Robin, J. P. Meirelis, *Corros. Eng. Sci. Technol.* **44**, 352 (2009).
- [26] Y. J. Bai, Y. B. Wang, Y. Cheng, F. Deng, Y. F. Zheng, S. C. Wei, *Mater. Sci. Eng. C* **31**, 702 (2011).

- [27] A. Kocijan, D. Kek Merl, M. Jenko, *Corros. Sci.* **53**, 776 (2011).
- [28] G. Bolat, D. Mareci, S. Iacoban, N. Cimpoesu, C. Munteanu, *J. Spectrosc.*, Article Number: 714920, DOI: 10.1155/2013/714920 (2013).
- [29] T. Fusayama, T. Katayori, S. Nomoto, *J. Dent. Res.* **42**, 1183 (1963).
- [30] G. Mabileau, S. Bourdon, M. L. Joly-Guillou, R. Filmon, M. F. Basle, D. Chappard, *Acta Biomater.* **2**, 121 (2006).
- [31] H. J. Mueller, Tarnish and corrosion of dental alloys. In: J. K. Lawrence, L. O. David editors, *Metals handbook* (vol. 13: Corrosion), 9th ed. Metals Park, OH: ASM International (1988).
- [32] D. Mareci, I. Rusu, R. Chelariu, G. Bolat, C. Munteanu, D. Sutiman, R. M. Souto, *EJST* **9**, 189 (2013).
- [33] Her-Hesiung Huang, Tzu-Hsin Lee, *Dent. Mater.* **21**, 749 (2005).
- [34] D. Mareci, D. Sutiman, R. Chelariu, F. Leon, S. Curteanu, *Corros. Sci.* **73**, 106 (2013).